

Available online at [www.sciencedirect.com](http://www.sciencedirect.com)

SciVerse ScienceDirect

Energy Procedia 25 (2012) 108 – 117

Energy  
Procedia

PV Asia Pacific Conference 2011

## Temporal and Spatial Variations of the Solar Radiation Observed in Singapore

Ramkumar Jayaraman<sup>a,\*</sup>, Douglas L. Maskell<sup>a</sup><sup>a</sup>*Nanyang Technological University, 50 Nanyang Avenue, Singapore 639798, Singapore*

---

### Abstract

Meteorological phenomena, such as fast moving clouds, cause rapid changes in the terrestrial direct beam radiation. This introduces transients in both the temporal and spatial measurements of global horizontal radiation. These transients in radiation affect the performance of solar energy conversion systems (PV, CPV systems and solar thermal applications) and cause their output power to vary widely. Thus, to properly understand the dynamic fluctuations observed in the output energies of large solar farms and PV arrays, it becomes necessary to perform a high-resolution temporal and spatial measurement of solar radiation. It turns out that performing such high-resolution measurements is often cost-prohibitive. Studies were conducted to understand and quantify the temporal and the spatial variations of direct beam, diffused and global horizontal radiation. These studies were based on the radiation data collected at the Nanyang Technological University, Singapore at a time interval of 1 s. It was inferred from these studies that the temporal variations in the instantaneous diffuse radiation are minimum and there was little spatial variations seen across distances of 500 m. The transients observed in global horizontal radiation are predominantly restricted to the changes occurring in the direct beam component of the solar radiation. Based on these inferences, a simple and cost-effective method is proposed that would permit accurate large scale localised high-resolution measurements of individual components of the solar radiation.

© 2012 Published by Elsevier Ltd. Selection and/or peer-review under responsibility of Solar Energy Research Institute of Singapore (SERIS) – National University of Singapore (NUS). The PV Asia Pacific Conference 2011 was jointly organised by SERIS and the Asian Photovoltaic Industry Association (APVIA).

Open access under [CC BY-NC-ND license](https://creativecommons.org/licenses/by-nc-nd/4.0/).

*Keywords:* PV variability; temporal variations; spatial variations; transients; high-resolution radiation measurements

---

---

\* Corresponding author. Tel.: +65 6790 6644; fax: +65 6792 0774

E-mail address: [ramkumarj@ntu.edu.sg](mailto:ramkumarj@ntu.edu.sg)

## 1. Introduction

It is well established that high resolution measurements of solar radiation components are required for characterising the potential of photovoltaic (PV), concentrated photovoltaic (CPV) and concentrated solar thermal (CST) applications. Measurements of the solar radiation components (i.e. direct beam, diffused and global horizontal) at Singapore has indicated that there are considerable transients in the insolation pattern due to local meteorological factors such as rapidly moving clouds. Transients in radiation of 50 W/m<sup>2</sup>s are common and transients of up to 300 W/m<sup>2</sup>s are observed based on past data measurements. These temporal transients are likely to significantly impact the efficiencies of solar energy conversion systems, in particular the PV and CPV systems [1, 2]. The impact on the efficiencies of such systems is in two ways. Firstly, PV and CPV systems require instantaneous values of solar radiation due to the non-linear and fast response times (of the order of  $\mu$ s) of the PV cell. Secondly, the temporal transients are likely to affect the dynamic performance of the charge controllers, which are commonly used in PV and CPV applications [3, 4]. Fast moving clouds also cause spatial variations in the solar insolation. Spatial variations in the solar radiation cause non-uniform illumination of large PV arrays thereby impacting their net conversion efficiencies. These factors (temporal transients and spatial variations) introduce variabilities in the output energies of large PV arrays and solar farms. Thus, it becomes necessary to perform a high-resolution temporal and spatial measurement of the solar radiation components for appropriately characterising the outputs from large PV and CPV systems. However, the costs associated with the tracking infrastructure (required for performing accurate measurements of direct beam and diffused radiation) and the instrumentation makes such field measurement expensive, prompting the use of alternate techniques and methodologies to gather the required data.

In this paper, we examine the use of a computationally simple and cost effective methodology for obtaining high-resolution temporal and spatial measurements of solar radiation with minimal field instrumentation. This method is likely to help engineers at solar farms in improving their understanding of the variabilities and fluctuations observed in the output power of the PV and CPV systems. This in turn helps to better manage problems in energy estimation, load scheduling and balancing.

The work done in this paper is organised as follows. Section 2 presents the literature survey where other techniques for estimating the solar radiation components with limited field measurements are presented. Section 3 discusses the short-term variability observed in the different components of solar radiation measured during August 2010 - January 2011. Section 4 provides details on the spatial correlation between the solar radiation components measured from two independent monitoring stations at a distance of about 500 m. Section 5 presents the methodology of estimating direct beam radiation from the measured global horizontal radiation and presents a comparison between the estimated and the measured values. Section 6 provides conclusion to this paper and discusses avenues for future work.

### Nomenclature

G(k)	Radiation measurement at k <sup>th</sup> instant, in W/m <sup>2</sup>
I(k)	Instantaneous difference of radiation at k <sup>th</sup> instant, in W/(m <sup>2</sup> s)
Z	Zenith angle of the sun

## 2. Literature survey

The estimation of diffused radiation from measured global horizontal radiation using correlation studies is a well-studied problem. The pioneering work on this was done by Liu and Jordan in Ref. [5]. Empirical correlation equations between the diffuse fraction and the clearness indices based on daily and monthly intervals of radiation data were derived in Ref. [5]. Similar work was done by Orgill *et al.* in Ref. [6] where hourly correlations between diffused fraction and clearness index were developed based on data from four independent solar monitoring stations. These empirical relations depart significantly from those provided in Ref. [5]. This highlights the localised validity of the empirical relations derived from correlation studies (However, this is not always true, see Ref. [7]). Iqbal [7] categorised the data from five solar monitoring stations (3 Canadian and 2 French stations) based on solar altitude angles and derived the empirical relations between clearness index and diffused factors. Similar correlation studies based on categorisation of data using other meteorological factors such as cloud cover in Ref. [8], sun shine duration in Ref. [9], seasonal variations in Ref. [10], albedo in Ref. [11] and water precipitation can be found in the literature.

Hollands [12] developed a theoretical derivation for the average diffuse fraction based on the clearness index, in which he characterised the atmosphere as two spectrally non-selective homogenous layers with the upper atmospheric layer contributing only to absorption and the lower atmosphere contributing to both absorption and scattering. The result from this theoretical model fits well with the empirical relations resulting from correlation studies in Ref. [6]. This theoretical model was extended further by including the effect of atmospheric back-scattering in Ref. [13].

A major drawback with the work done in Ref. [5-13], is that the radiation measurements used for the studies have sampling intervals between an hour to a month. It has been established in Ref. [2] and Ref. [14] that the use of diffused fractions derived from hourly correlation studies introduces significant inaccuracies in the prediction of the performance of solar energy conversion systems where short-term variability (of the order of few minutes or less) in the solar radiation is observed. This error is due to the fast response time and non-linearity associated with the solar energy conversion system. These observations are likely to be valid in Singapore where significant variations in insolation between consecutive seconds are not uncommon. Thus, methodologies presented in Ref. [5-13] cannot be utilised for accurately predicting the diffuse radiation from the field measurements of global horizontal radiation (and other meteorological parameters).

The strong dependency between the diffused fraction (based on short-term radiation data) and the air-mass index is witnessed in Ref. [14] and Ref. [15]. Suehrcke has derived regression equations between one-minute diffuse fraction and one-minute clearness indices which in turn are a function of air-mass indices [15]. Similar work has been done by Gayathri *et al.* in Ref. [14] where one- and three-minute radiation data measured at three independent stations followed similar dependence on air-mass index as observed in Ref. [15]. Thus, the diffused radiation can be determined from the measured global horizontal and air-mass indices. Air-mass indices can be determined accurately by evaluating the position of the sun for the given time of day.

## 3. Temporal variations in direct beam, diffused and global horizontal radiation

Measurements of direct beam, diffused and global horizontal radiation were carried out at Nanyang Technological University (Latitude: 1.34 N, Longitude: 103.68E) at a sampling rate of 1 Hz. The

specifications of the instrumentation and the solar tracking system used for carrying out these measurements are provided in Table 1. The radiation data measured for a period of six months (from 1 August 2010 to 31 January 2011) is used for quantifying the temporal variations in the different components of solar radiation.

Table 1. Specifications of instrumentation and solar tracker used for the radiation measurements

Sensor / Tracker	Specifications
K&Z CHP-1 pyrheliometer	Response time (for 95% response) : 5 s FOV : 5 degree
K&Z CMP-11 pyranometer with shading ball assembly	Response time (for 95% response) : 5 s FOV : 180 degree (shading ball blocks the 5 degree around the solar disk for diffused measurements)
K&Z CMP-11 pyranometer	Response time (for 95% response) : 5 s FOV : 180 degree
K&Z SOLYS-2 sun tracker	Tracking accuracy : 0.1 degree, BSRN-level of performance

Instantaneous differences in the direct beam, diffused and global horizontal radiation were calculated for the radiation data that cleared quality control (7894683 samples were considered after quality checks). The instantaneous differences were calculated using Eq. (1).

$$I(k) = |G(k+1) - G(k)| \quad (1)$$

where  $I(k)$  represents the instantaneous difference in  $W/(m^2 s)$  and  $G(k)$  represents the radiation at the  $k$ th second in  $W/m^2$

The distribution of the instantaneous differences between the per-second values of direct beam, diffused and global horizontal radiation are provided in Table 2 and 3. The maximum rate of change in the transients observed in the direct beam, diffused and global horizontal radiation is found as  $361 W/m^2s$ ,  $50 W/m^2s$  and  $369 W/m^2s$  respectively.

From Table 2, it can be observed that there are only about 2% of instantaneous radiation differences (for direct beam and global horizontal) in the range of  $> 25 W/m^2s$ , while the majority falls in the range of  $< 25 W/m^2s$ . Such an analysis interprets the probability of transient occurrence with ramp rate  $> 25 W/m^2s$  to be negligible ( $\sim 0.0132$  for direct beam and  $\sim 0.0108$  for global horizontal radiation). This does not however mean that the effects of such transients on solar energy conversion systems can be ignored. The solar energy conversion system does not work at its best efficiency for a significant portion of the steady-state conditions following a transient [16-18]. This is especially true for PV and CPV systems where the charge controller has to track a new maximum power point as a result of the rapid change in the insolation (The ability to track the maximum power point in response to a rapid change in radiation depends on the type of the MPPT algorithm used in the charge controller. There are many trade-offs such as speed of convergence, stability, ease of implementation and sensor costs in selecting the ideal MPPT algorithm which are discussed in Ref. [18]).

Table 2. Distribution of the temporal changes in the direct beam and global horizontal radiation

Range of the instantaneous differences (W/m <sup>2</sup> s)	Number of occurrences of direct beam differences	Percentage of occurrences of direct beam differences	Number of occurrences of global horizontal differences	Percentage of occurrences of global horizontal differences
0 - 25	7790650	98.68	7809048	98.92
25 - 50	64357	0.8050	54486	0.69
50 - 75	20928	0.2648	17135	0.22
75 - 100	9435	0.1192	7390	0.094
100 - 125	4641	0.0587	3499	0.044
125 - 150	2343	0.0297	1619	0.021
150 - 175	1148	0.0145	780	0.0099
175 - 200	600	0.0076	385	0.0049
Above 200	581	0.0074	342	0.0043

Table 3. Distribution of the temporal changes in the diffused radiation

Range of the instantaneous difference for diffused radiation (W/m <sup>2</sup> s)	Number of occurrences	Percentage of occurrences
0 - 25	7794679	99.999
Above 25	5	0.000063

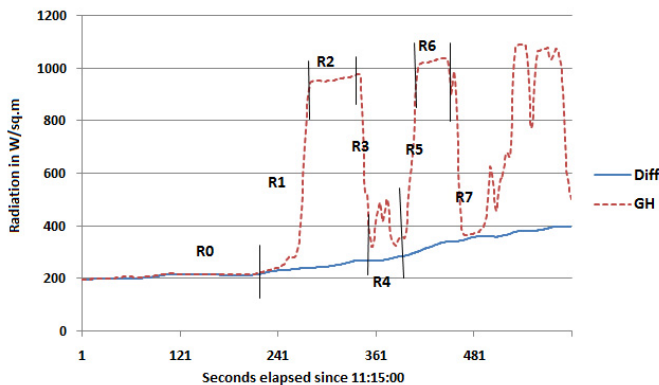


Fig. 1. Variations in diffused and global horizontal radiation observed between 11:15 and 11:24 on 1 September 2010

Figure 1 shows the variation in the global horizontal and diffused radiation observed over a 10-minute period between 11:15:00 and 11:24:59 on 1 September 2010. The variations in the global horizontal radiation in Fig. 1, is divided into eight regions and is marked by R0 to R7. The characteristics of global horizontal radiation in these regions are provided in Table 4. From Table 4, we can observe that most transients are preceded and followed by a period of (reasonably) steady state conditions. For instance, the steady state region R2 is preceded and followed by transient conditions marked by regions R1 and R3. For a significant amount of time (depending on the MPPT algorithm used) during the steady state condition (i.e. regions R2, R4 and R6), the charge controllers work at lower efficiencies due to the inability of the controller algorithm to accurately track the sudden change in insolation [17, 18]. Thus, the effect of the

transients on solar energy conversion systems is not restricted to just the period of their occurrence, but also during the steady-state insolation condition (which follows the transients).

R3 corresponds to a fall in global horizontal radiation from  $958 \text{ W/m}^2$  to  $320 \text{ W/m}^2$  in about 15 s. The instantaneous differences corresponding to R3 are 16.47, 43.93, 63.95, 78.94, 114.53, 87.41, 45.42, 8, 2, 57.90, 56.63, 29.63, 22.65, 18.54 and  $11.32 \text{ W/m}^2\text{s}$ . It can be observed that even a steep transient (such as R3 with an average ramp rate of  $42.5 \text{ W/m}^2\text{s}$ ) can consist of significant steady-state components. Thus, it can be concluded that the frequency distribution studies (given in Table 2 and 3) can only provide probabilities for the instantaneous changes in radiation but not for the occurrences of transients. The occurrence of a transient is a purely meteorological phenomenon with the shape, type, height and the velocity of the cloud affecting the instantaneous value of direct beam radiation (and hence the global horizontal) during the cloud pass.

Table 4. Characteristics of temporal variations in global horizontal observed on 1 September 2010 between 11:15:00 and 11:24:59

Region in Fig. 1	Characteristics of observed global horizontal radiation
R0	Steady-state, about $\sim 250 \text{ W/m}^2$ and lasts for 265 s
R1	Transient increasing from $300 \text{ W/m}^2$ to $900 \text{ W/m}^2$ in 14 s
R2	Steady-state about $\sim 950 \text{ W/m}^2$ and lasts for 63 s
R3	Transient falling from $958 \text{ W/m}^2$ to $320 \text{ W/m}^2$ in 15 s
R4	Approximated as a steady-state region with minor transients
R5	Transient increasing from $350 \text{ W/m}^2$ to $970 \text{ W/m}^2$ in 16 s
R6	Steady-state, about $\sim 1050 \text{ W/m}^2$ and lasts for 40 s
R7	Not studied

From Table 3, it can be observed that the variations in diffused radiation are small (98.45% of changes in diffused radiation are observed under  $1 \text{ W/m}^2\text{s}$ ) and almost all variations in the diffused radiation occur within  $25 \text{ W/m}^2\text{s}$ . This signifies the slow varying nature of the diffused radiation which is also evident from Fig. 1.

#### 4. Spatial variations in direct beam, diffused and global horizontal radiation

To establish the spatial variations in the direct beam, diffused and global horizontal radiation, measurements from a neighbouring solar monitoring station (located at a distance of 500 m) are compared with the data measurements from the primary station. Radiation data from the neighbouring station is available in intervals of 1 minute. The comparison is made by super-imposing about 2 months of data (As Singapore lies in the tropics, the climate is similar all year round. The two months of radiation data i.e. Sept-2010 to Oct-2010 is considered to be reasonably representative of the full year) collected from the neighbouring station on the data from the primary station and finding the root-mean square error (RMSE) and the R-coefficient. Figure 2(a) shows the results of comparison between the diffused radiation from the two stations recorded on 14 September 2010. It is evident from the Fig. 2(a) that the diffuse radiation collected from the two stations match well. The RMSE and R-coefficient for the two sets of diffused radiation recorded on 14 September 2010 is  $0.8818 \text{ W/m}^2$  and 0.9909. Figure 2(b) provides the RMSE and the R-coefficient for the diffused radiation measurements from the two stations during the months of September 2010 and October 2010. The worst-case values of RMSE and R-coefficient for this set of diffused radiation data are  $3.5 \text{ W/m}^2$  and 0.938 respectively. Thus, it can be concluded that the diffused radiation can be assumed uniform over spatial distances of 500 m within a reasonable degree of accuracy.

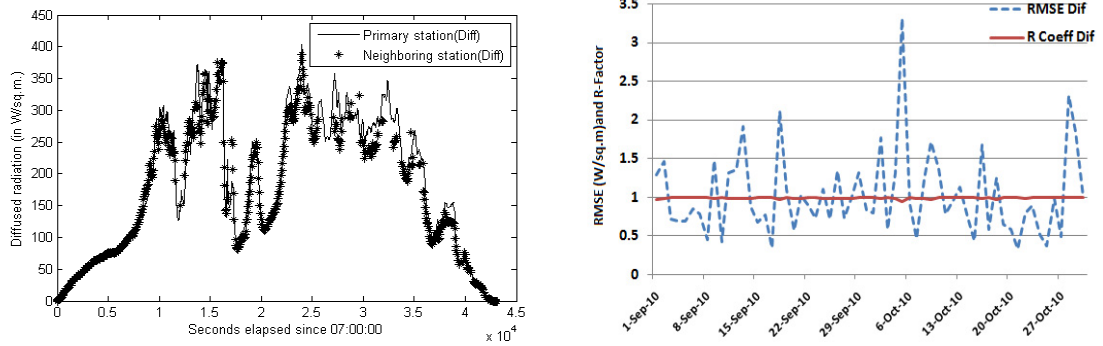


Fig. 2. (a) Spatial variations observed in the diffused radiation measurements from the two stations on 14 September 2010 between 07:00 and 18:59; (b) RMSE and R-coefficient for the diffused radiation measurements from the two stations for months of September 2010 and October 2010

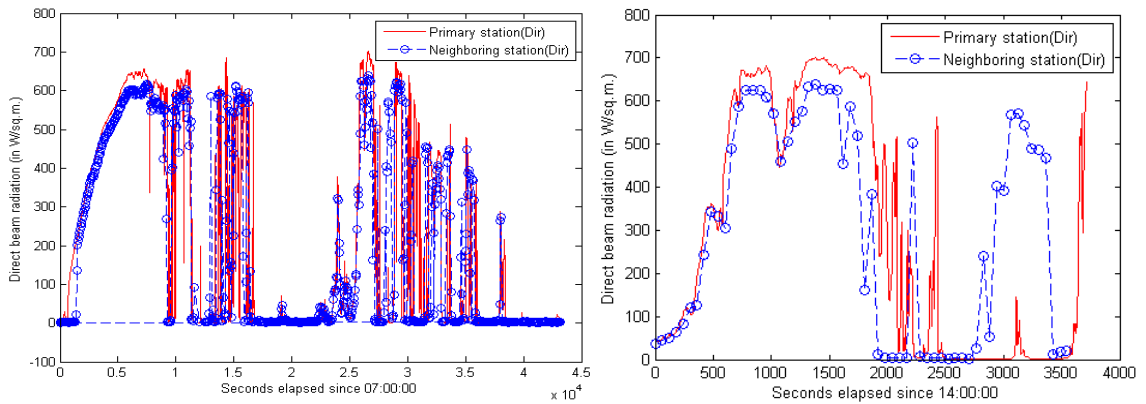


Fig. 3. (a) Spatial variations between the direct beam measurements from the two stations on 14 September 2010 between 07:00 and 18:59; (b) Comparison between the direct beam measurements from the two stations on 14 September 2010 between 14:00 and 14:59

Figure 3(a) shows the results of comparison between the direct beam measurements from the two stations recorded on the 14 September 2010. The RMSE and R-coefficient for this comparison on 14 September 2010 is  $6.424 \text{ W/m}^2$  and  $0.7869$ . It can be observed from Fig. 3(a) that the direct beam radiation measured at the neighbouring station stays at zero around sunrise and sunset times, whereas the direct radiation sensor at the primary stations records non-zero and positive values. This is due to the difference in elevation of the two monitoring stations. Except for these minor differences which occur at low solar elevation angles, the direct beam radiation measurements from the two stations resemble each other. However when transients occur, significant differences in the direct beam radiation are observed. This is shown in Fig. 3(b). A comparison of direct beam measurements from the two stations for a period of 1 hour (i.e. 14:00 to 14:59 on 14 September 2010) is presented in Fig. 3(b). It can be observed that there are many instances where the direct beam measurements on the primary station is close to zero but the measurements from the neighbouring station exceeds  $500 \text{ W/m}^2$  and vice-versa. This confirms that the spatial variations in the direct beam radiation are common and significant.



Figure 4(a) provides the results of comparison between the global horizontal radiation from the two stations recorded on the 14 September 2010. The RMSE and R-coefficient this comparison on 14 September 2010 is  $5.602 \text{ W/m}^2$  and 0.8304.

From Fig. 3(b) and Fig. 4(b), it is evident that the spatial differences in the global horizontal radiation are in fact the spatial differences observed in the direct beam radiation. The diffused radiation stays uniform over distances of 500 m. The curve given in Fig. 4(b) can be treated as an upward shifted version (shifted towards positive Y-axis infinity) of the curve in Fig. 3(b) with the diffused radiation determining the extent of the shift.

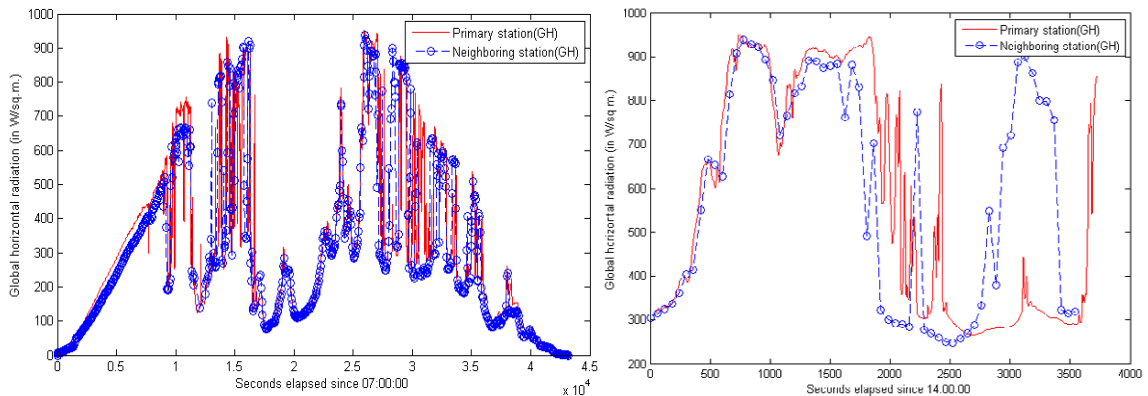


Fig. 4. (a) Comparison between the global horizontal radiation measurements from the two stations on 14 September 2010 between 07:00 and 18:59; (b) Comparison between the global horizontal radiation measurements from the two stations on 14 September 2010 between 14:00 and 14:59

## 5. Estimation of direct beam radiation from global horizontal measurements

Having established that the diffused radiation changes slowly and can be assumed constant within distances of 500 m, the direct beam radiation can be estimated from the field measurements of global horizontal radiation with the values of diffused radiation from a neighbouring monitoring station. Unlike the direct beam and/or diffused radiation measurements which need tracking capabilities and/or shadow bands or occulting disks, field measurements of global horizontal are simple, straightforward and inexpensive. Thus, this method can be employed in solar farms where a single monitoring station in conjunction with multiple global horizontal sensors can be used in performing high-resolution temporal and spatial measurements. It is also possible to further reduce the cost of instrumentation by using low-cost silicon sensors to perform the global horizontal measurements in place of thermopile instruments, if the measurement errors can be tolerated or corrected.

The interrelationship between the direct beam, diffused and global horizontal radiation is given in Eq. (2) [19]. Equation (2) can be used in evaluating the direct beam radiation from field measurements of global horizontal radiation using the diffused radiation measurements from a neighbouring station.

$$\text{Global Horizontal} = (\text{Direct Beam} * \text{Cos } Z) + \text{Diffused radiation} \quad (2)$$

where  $Z$  is the zenith angle of the sun.



Table 5. Comparison drawn between the direct beam radiation from primary station, measured direct beam at neighbouring station and calculated direct beam at neighbouring station based on data recorded on 1 September 2010 between 12:00 and 14:59

Comparison drawn between	RMSE ( $\text{W}/\text{m}^2$ )	R-coefficient
Direct beam measured from primary station and neighbouring station	15.43	0.7908
Direct beam measured at neighbouring station and the calculated values of direct beam from GH at neighbouring station and diffused radiation from primary station	2.96	0.9979

To verify the level of accuracy of the direct beam radiation evaluated from this method, diffused radiation from the primary monitoring station and global horizontal measurements from the neighboring station collected on 01 September 2010 between 12:00 and 14:59 are used to derive the direct beam radiation at the neighbouring station. The calculated values of the direct beam radiation are then compared with the actual observed values. The results of this comparison are provided in Fig. 5 and Table 5. From Table 5, it can be observed that the direct beam measurements from the primary and neighbouring station differ significantly. With the field measurements of global horizontal radiation and the diffused radiation readings from a nearby site, the direct beam radiation can be calculated to a sufficient degree of accuracy which matches well with the measured values.

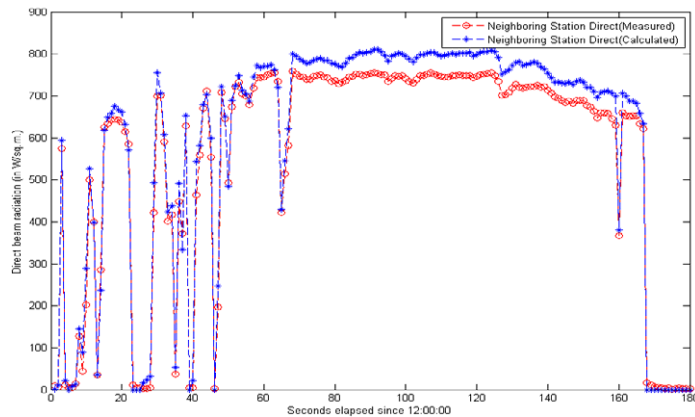


Fig. 5. Comparison between the measured and calculated values of the direct beam radiation at the neighbouring station on 01 September 2010 between 12:00 and 14:59

## 6. Conclusion

Measurements of direct beam, diffused and global horizontal radiation at Singapore indicates the presence of transients in the insolation pattern. It is found that these transients vary temporally as well as spatially. This paper presents the characteristics of the temporal and the spatial variations observed in the different components of solar radiation measured in Singapore. The direct beam and global horizontal radiation exhibit rapid changes due to fast moving clouds. Temporal changes with ramp rates of up to  $300 \text{ W}/\text{m}^2\text{s}$  are observed based on the radiation measurements. However, it has been found that the temporal changes in the diffused radiation are very minimal. Studies were then conducted to ascertain the spatial variations in the components of radiation; by comparing the direct beam, diffused and global horizontal measurements between two independent stations at a distance of 500 m. It has been observed that there are significant differences in the direct beam and global horizontal measurements from the two stations. The diffused radiation however is uniform across distances of  $\sim 500 \text{ m}$ . Based on the observation that the

diffused radiation is uniform spatially and slow varying temporally, we present a simple and cost-efficient methodology for performing high-resolution temporal and spatial measurements of solar radiation with minimal field instrumentation. It has been demonstrated that direct beam radiation can be estimated to a reasonable degree of accuracy based on this methodology. Future work would be focused on further reducing the cost of instrumentation by replacing the thermopile instruments with corrected low-cost silicon sensors. Thus, by installing multiple low-cost silicon sensors along with a single solar monitoring station we should be able to generate sufficiently accurate temporal and spatial maps of rapidly changing solar insolation with reduced instrumentation costs.

## Acknowledgements

We thank Y. Shineng and C.F. Hoong from School of EEE, NTU for the data from the neighboring station. We acknowledge the support from the Singapore National Research Foundation, grant no. NRF2008EWT-CERP02-025.

## References

- [1] Tovar J, Olmo FJ, Alados-Arboledas L. One-minute global irradiance probability density distributions conditioned to the optical air mass. *Solar Energy* 1998; **62(6)**:387-93.
- [2] Gansler RA, Klein SA, Beckman WA. Investigation of minute solar radiation data. *Solar Energy* 1995;**55(1)**:21-7.
- [3] Bründlinger R, Henze N, Häberlin H, Burger B, Bergmann A, Baumgartner F. prEN 50530 – The New European Standard for Performance Characterisation of PV Inverters. *Proc. 24<sup>th</sup> European Photovoltaic Solar Energy Conf., Hamburg, Germany*; 2009, p. 3105-9.
- [4] Haeberlin H, Schaerf P. New Procedure for Measuring Dynamic MPP-Tracking Efficiency at Grid-Connected PV Inverters. *Proc. 24<sup>th</sup> European Photovoltaic Solar Energy Conf., Hamburg, Germany*; 2009, p. 3631-7.
- [5] Liu BYH, Jordan RC. The interrelationship and characteristic distribution of direct, diffused and total solar radiation. *Solar Energy* 1960;**4(3)**:1-19.
- [6] Orgill JF, Hollands KGT. Correlation equation for hourly diffuse radiation on a horizontal surface. *Solar Energy* 1977;**19(4)**:357-9.
- [7] Iqbal M. Prediction of hourly diffuse solar radiation from measured hourly global radiation on a horizontal surface. *Solar Energy* 1980;**24(5)**:491-503.
- [8] Castagnoli C, Giraud C, Longhetto A, Morra O, Civitano L. Correlation between normal and direct radiation and global radiation depending on cloudiness. *Solar Energy* 1982;**28(4)**:289-92.
- [9] Hussain M. Correlating beam radiation with sunshine duration. *Solar Energy* 1992;**48(3)**:145-9.
- [10] Chang J. Diffuse radiation as related to global radiation and the Angot value. *Theoretical and Applied Climatology* 1980;**28(1-2)**:31-9.
- [11] Lestrade JP, Acock B, Trent T. The effect of cloud layer plane albedo on global and diffuse insolation. *Solar Energy* 1990;**44(2)**:115-21.
- [12] Hollands KGT. A derivation for diffuse fraction's dependence on the clearness index. *Solar Energy* 1985;**35(2)**:131-6.
- [13] Hollands KGT, Crha SJ. An improved model for diffuse radiation : correction for atmospheric back-scattering. *Solar Energy* 1987;**38(4)**:233-6.
- [14] Vijayakumar G, Kummert M, Klein SA, Beckman WA. Analysis of short-term solar radiation data. *Solar Energy* 2005; **79(5)**:495-504.
- [15] Suehrcke H, McCormick PG. The diffuse fraction of instantaneous solar radiation. *Solar Energy* 1988;**40(5)**:423-30.
- [16] Eck M, Hirsch T. Dynamics and control of parabolic trough collector loops with direct steam generation. *Solar Energy* 2007;**81(2)**:268-79.
- [17] Bletterie B, Bruendlinger R, Spielauer S. Quantifying dynamic MPPT performance under realistic conditions first test results - the way forward. *Proc. 21<sup>st</sup> European Photovoltaic Solar Energy Conf., Dresden, Germany*; 2006, p. 2347.
- [18] ESRAM T, Chapman PL. Comparison of photovoltaic array maximum power point tracking techniques. *IEEE Trans. Energy Conversion* 2007;**22(2)**:439-49.
- [19] McArthur LJB. Baseline Surface Radiation Network (BSRN) Operations Manual v.2.1. World Climate Research Programme.